Magnetic anistropy in ultrathin epitaxial Fe/Ag(100) films with overlayers

R. J. Hicken,* S. J. Gray, A. Ercole, C. Daboo, D. J. Freeland, E. Gu, E. Ahmad, and J. A. C. Bland
Cavendish Laboratory, Madingley Road, Cambridge CB3 0HE, United Kingdom
(Received 29 March 1996; revised manuscript received 31 October 1996)

In situ Brillouin light-scattering and magneto-optical Kerr effect measurements have been used to determine the values of the magnetic anisotropy constants in ultrathin epitaxial Fe/Ag(100) films both during the deposition of the Fe layer and also during the deposition of overlayers of Ag and Cr. The structural properties of the films have been investigated by means of reflection high-energy electron diffraction and low-energy electron diffraction. We show that the values of the cubic magnetocrystalline anisotropy constant K_1 and the magnetic surface anisotropy constant K_s are strongly dependent upon the value of the Fe layer thickness d, and that they differ in sensitivity to the surface structure of the substrate. We find that the thickness of a Ag or Cr overlayer must be at least 3 ML thick before the value of K_s is saturated. Cr and Ag capping layers are found to have a qualitatively different effect upon the magnetic anisotropy which we attribute to the presence of magnetic order in the Cr. [S0163-1829(97)02409-0]

I. INTRODUCTION

Magnetic anisotropy plays a key role in the physics of ultrathin magnetic structures since it affects the orientation of the magnetization, the nature of the domain walls, the frequencies of spin-wave excitations, and consequently the thermodynamic behavior of the film. For an itinerant ferromagnet such as Fe the anisotropy is sensitively dependent upon the electronic band structure of the film and it remains a challenge to both experimentalists and theorists to determine the way in which modified lattice structure, reduced dimensionality, or the presence of interfaces affect the anisotropy. It has frequently been assumed that the total magnetic anisotropy energy can be divided into a volume energy term and a surface energy term, introduced by Néel,[1] and that these energies are independent of the film thickness. However, recent work now provides evidence that both surface and volume anisotropies may have a marked thickness dependence.[2–4] To further explore such behavior we have studied the dependence of the cubic magnetocrystalline anisotropy energy and the uniaxial perpendicular surface anisotropy energy upon the thicknesses of both the Fe film and that of an overlayer material in the model system of Fe/Ag(100). We have used *in situ* Brillouin light scattering (BLS) to study, first, films of different Fe thickness d, grown upon identical substrates; second, the Fe/vacuum interface; and third, Fe films with ultrathin overlayers. *In situ* BLS allows the anisotropy to be measured sufficiently quickly that no significant surface contamination occurs before deposition of the film is resumed. We have studied the effect first of Ag overlayers which yield symmetric boundary conditions, and second of Cr overlayers since Cr is known to mediate an oscillatory interlayer exchange coupling in Fe/Cr/Fe trilayers[5] and because a layered antiferromagnetic order has been reported for the Cr layer,[6,7] which may be frustrated by surface roughness.[8] We will show: first, that for Fe/Ag(100) both the cubic and surface anisotropies are strongly dependent upon both the Fe layer thickness and the detailed preparation of the substrate; second, that the surface anisotropy energy continues to change until 3 ML of overlayer have been deposited; and third, that the effects of Ag and Cr overlayers upon the surface anisotropy are in fact qualitatively different. In the remainder of the Introduction we describe recent work relevant to both the structural and magnetic properties of these ultrathin film structures. In Sec. II we describe the *in situ* BLS experiment and describe how it is used to quantify the anisotropy. Section III presents details of the growth and structural characterization of our films, while Sec. IV considers the variation of anisotropy with Fe thickness. Overlayer experiments are discussed in Sec. V, and then we conclude with a discussion of all of our results in Sec. VI.

It is expected that bcc Fe will grow epitaxially on the (100) face of fcc Ag since the lattice parameter of bulk Fe (2.87 Å) is just 0.8% smaller than the nearest-neighbor separation in bulk Ag. Also Fe and Ag are known to be immiscible in the bulk so limited interfacial diffusion is expected. Since Fe has a surface energy roughly twice that of Ag,[9,10] thermodynamic arguments suggest[11] that Ag should wet Fe but that Fe should not wet Ag. This ignores the inequivalence of different surface sites, such as those at step edges, and assumes that surface atoms can locate a minimum energy state. For growth at room temperature distinct breaks are seen in recorded Auger intensities[12,13] for the first 3 ML of Fe but the $p(1\times1)$ low-energy electron diffraction (LEED) pattern is significantly broadened at 3 ML (Refs. 12–18) before reappearing for larger Fe thicknesses. One LEED $I(V)$ study[16] suggested that for $d<3$ ML the LEED pattern is due to exposed Ag while a second[19] suggested that the pattern results from the Fe film for $d\geqslant2$ ML. Recently Mössbauer spectroscopy has confirmed[20] that the initial growth of Fe is three dimensional and, while about 0.1 ML of Fe interdiffuses with the Ag substrate, no interdiffusion occurs during the deposition of Ag onto Fe. Studies of Fe/Ag superlattices grown on Ag/NaCl(100) confirm that the Fe/Ag and Ag/Fe interfaces are not identical and indicate a tetragonal distortion of the Fe atoms at the interfaces.[21] X-ray photoelectron and Auger electron forward scattering[22] also suggest some initial interdiffusion for the growth of Fe on Ag(100) that leads to the first few monolayers being highly

strained. Reflection high-energy electron-diffraction (RHEED) patterns from Fe films are found to be broader than those from a bulk Ag(100) substrate[23] and Henzler streak splittings indicate an island separation of about 60 Å on the Fe surface.[24] The amplitude of the RHEED oscillations is uncertain for the first 3 or 4 ML of Fe,[20,25–27] which may occur if the step separation is less than 120 Å.[24]

Results from the homoepitaxial growth of Fe onto Fe whisker substrates may be relevant to Fe/Ag(100) once full Fe coverage of the Ag is obtained. The amplitude of RHEED intensity oscillations was found to be a maximum at grazing incidence and at the anti-Bragg condition, but to decrease with increasing temperature and film thickness.[28] Combined scanning tunneling microscope and RHEED studies[29,30] have shown that at room temperature up to 5 ML of Fe may be simultaneously exposed compared to 3 ML at 250 °C. In the latter case the RHEED patterns were sharper with no Henzler streak splitting and although the amplitude of the oscillations was reduced, they were less heavily damped. For temperatures above 250 °C the Fe surface was observed to coarsen.[29] Following the surprising observation of highly damped RHEED intensity oscillations for the growth of Fe on Ag(100) at liquid-nitrogen temperature,[31] transient surface diffusion of Fe atoms[31] and a ''funneling down'' growth mechanism[32,33] were proposed. Recent experiments[34,35] at various temperatures have yielded scaling relations for the size of the islands on the Fe surface, while recent simulations take the effects of both step-edge barriers and funneling down into account.[36]

The growth of Fe on Ag differs from the homoepitaxial growth of Fe in that interfacial diffusion may occur at elevated growth temperatures. Photoemission studies showed negligible interdiffusion for post-deposition annealing below 200 °C,[18,37] but recent reports[38] suggest that 0.2 and 1.2 ML thick layers of Ag may float on top of the Fe layer for growth at room temperature and 250 °C, respectively. If the first 5 ML of Fe is grown at room temperature then subsequent growth at and above 410 K gives sharp RHEED patterns with no Henzler streak splitting and larger amplitude RHEED intensity oscillations.[24] While it was reported[39] that a 30 min post-deposition anneal at 150 °C sharpens both RHEED and LEED patterns from Fe/Ag(100), this was not corroborated by annealing studies[24] at up to 510 K. It seems that even after the Ag is fully covered with Fe there is no growth temperature for which the Fe surface is atomically flat although the use of surfactants such as oxygen[19] has yet to be fully explored.

Fe/Ag(100) is a model system for theoretical studies of magnetism in ultrathin films. Since the *d* bands of Fe and Ag do not overlap and since the Ag *sp* bands are only weakly populated, Fe/Ag(100) is a close approximation to a free standing Fe film. Enhanced moments have been predicted for the Fe/vacuum and Fe/Ag interfaces,[40,41] and observed for Fe/Ag(100) structures capped with Ag, Au, Cu, and Pd.[42–44] A quasilinear temperature dependence of the magnetization has been observed at low temperatures[21,42–44] due to the two-dimensional nature of these structures while the Curie temperature may depend upon the temperature at which the films are grown.[45]

Spin-polarized angle-resolved photoemission spectroscopy studies[15] showed that a 2.5 ML Fe film had a spin-split electronic structure but no in-plane magnetization. The existence of perpendicular magnetization was confirmed by spin-polarized photoemission spectroscopy,[37] and by Mössbauer studies of Fe/Ag superlattices.[46] The origin of the perpendicular magnetization is the strong magnetic interface anisotropy, values for which were calculated from first principles[47] and measured by ferromagnetic resonance (FMR).[23] These studies[23] revealed that the surface anisotropy constant, the cubic anisotropy constant, and the FMR linewidth all depend upon the film thickness. Indeed these quantities also depend upon the substrate quality and the growth temperature[45] with maximum surface anisotropy constants of 0.96, 0.81, and 0.47 erg/cm^2 being reported for the Fe/vacuum, Fe/Ag, and Fe/Au interfaces, respectively.[3] A value of 0.8 erg/cm^2 was also observed at helium temperatures for Fe/Ag(100) superlattices grown on a Ag buffer layer on a GaAs(100) substrate.[48] The surface anisotropy constant for the Fe/vacuum interface can be increased by post-deposition annealing[39] but it is dramatically reduced by the adsorption of submonolayer quantities of oxygen.[19] Real ultrathin films generally have a tetragonal distortion normal to the film plane due to the imperfect lattice match with the substrate. This leads to a modification of the magnetocrystalline anisotropy such that two constants, $K_1^{\parallel}$ and $K_1^{\perp}$ are required to describe the in-plane and out-of-plane parts, respectively, of the fourth-order volume anisotropy. For Fe/Ag(100) the field associated with the perpendicular component, $2K_1^{\perp}/M$, in which M is the magnetization, was found[3] to change sign at $d=13$ ML, obtaining a value of -0.8 kOe at $d=3$ ML. The in-plane component was found to have the form $2K_1^{\parallel}/M=[0.55-2.5/d(\text{Å})]$ kOe and to be insensitive to the material used to cap the film, although if a layer of different material were placed between the Fe film and the Ag substrate a significant change was observed.[49]

For the vacuum/Fe/Ag(100) structure the value of d at which the magnetization switches from the out-of-plane to the in-plane configuration at room temperature has been reported to lie between 3 and 7 ML.[13,19,39] The critical thickness for this reorientation phase transition (RPT) becomes larger as the temperature is reduced. The RPT may be driven by changes in either the temperature, film thickness, or applied field strength, and theoretical studies have considered the entropy[50] and spin-wave spectrum[51,52] of the system, while renormalization-group[53] and Monte Carlo techniques[54] have been applied. For values of d and T just below the critical values there is an apparent loss of long-range magnetic order.[39,55] This may be explained by the presence of stripe domains with perpendicular magnetization[56–59] and similar domains are to be expected when the magnetization is forced into the plane by an applied field.[52] Calculations have also predicted a canted state,[60,61] but higher-order anisotropies must also be taken into account.[62] Clearly one must fully characterize the magnetic anisotropy present if one is to fully understand the RPT.

The effect of adding overlayers to magnetic films is currently of great interest. Quantum well states have already been observed in Ag overlayers[63] and they can cause the magnetic susceptibility of the overlayer to have an oscillatory thickness dependence.[64] There is evidence[7] that overlayers of Cr on Fe possess large magnetic moments and that a defect in the 2 ML period antiferromagnetic order may occur

within the first two ML of Cr at the interface. The effects of interdiffusion[65,66] and roughness of the Fe surface[8] must however be considered. The interface anisotropy is a quantity that is sensitive to both structural and electronic modification of the surface. Experiments in which a few ML of materials such as Cu, Ag, Au, and Pd have been added to Co films have shown that the interface anisotropy has a nonmonotonic dependence upon the overlayer thickness with an extremum occurring for a coverage of approximately 1 ML,[67–70] which is when the interfacial electronic structure becomes established. It is an open question as to what happens in the case of Fe rather than Co films, and we also address this issue in this paper.

II. EXPERIMENT

An important feature of our ultrahigh vacuum (UHV) deposition system is that the magnetic properties of the sample may be characterized *in situ*, during growth, by means of the magneto-optical Kerr effect (MOKE) and BLS. Optical techniques are well suited for use in vacuum systems and MOKE is rapidly becoming one of the most popular techniques for the *in situ* evaluation of magnetic properties. There have however been fewer reports of *in situ* BLS studies[71] probably because of three main technical difficulties that need to be overcome. First, the objective lens must subtend a reasonably large solid angle at the sample if sufficient signal is to be obtained. Second, measurements at any stage in the growth must be performed quickly in order that there is no significant contamination of the exposed film surface. Third, the BLS apparatus is sensitive to both mechanical vibrations and temperature variations of which any vacuum system is a strong source. We have employed a design[72] that overcomes these difficulties. Rather than moving the sample to a viewport for the BLS measurements, the objective lens is mounted in a reentrant tube on a bellows with a stepper motor drive which can be quickly moved close to the main sample position where we can also perform evaporation of two different materials, RHEED and MOKE measurements. A digital control system[73] allows optimum alignment of the interferometer to be quickly achieved. Finally, in order to achieve environmental isolation the growth chamber and the BLS apparatus are located in different rooms with a small hole in the laboratory wall allowing light to pass between the two. The magnet field for the BLS experiments is provided by a moveable Fe core electromagnet with a single layer of coils that can provide a maximum field of 2.2 kOe. Longitudinal MOKE measurements are made with the same configuration of sample and magnet. The MOKE beam enters and leaves the chamber through viewports that are well removed from the sample position in order to avoid any field-dependent birefringence.

It is expected from the fourfold structural symmetry of the Fe/Ag(100) system that the magnetic in-plane anisotropy will be predominantly fourfold and indeed from our accumulated MOKE and BLS measurements we have been unable to resolve any significant uniaxial in-plane anisotropy component. If the Fe(100) film is uniformly magnetized then we may write the magnetic free energy per unit area in the form

$$E = d\left[-\mathbf{M}\cdot\mathbf{H} - \frac{K_1^{\parallel}}{2}(u_y^4+u_z^4) - \frac{K_1^{\perp}}{2}u_x^4 + 2\pi D M^2 u_x^2 \right] + (K_s^{(1)}+K_s^{(2)})u_x^2, \quad (1)$$

in which u_x, u_y, and u_z are the direction cosines of the magnetization **M** relative to the crystallographic axes of the film, with the x axis being taken as the surface normal. **H** is the applied magnetic field vector, $K_1^{\parallel}$ and $K_1^{\perp}$ are the magnetocrystalline volume anisotropy constants as discussed earlier, and $K_s^{(1)}$ and $K_s^{(2)}$ are the surface anisotropy constants for the two surfaces of the film. A factor D has been included in the demagnetizing energy term to take into account the reduced demagnetizing field that occurs in ultrathin films due to the discrete nature of the lattice. We have taken D to have the form $1-0.425/N$ where N is the thickness of the Fe film in monolayers.[3,74] We have not included a volume-type uniaxial perpendicular anisotropy energy in Eq. (1) because this is believed to be small for Fe/Ag(100).[3]

All of the films to be considered in this study are sufficiently thin that the static magnetization can be considered to be uniform through the thickness of the film. In this case it is useful to define the effective demagnetizing field as

$$(4\pi M)_{\text{eff}} = 4\pi D M - 4K_s/Md, \quad (2)$$

in which $K_s=(K_s^{(1)}+K_s^{(2)})/2$ is the average surface anisotropy constant. Normally the perpendicular second-order uniaxial anisotropy energy dominates the fourth-order magnetocrystalline anisotropy terms so that if $(4\pi M)_{\text{eff}}>0$ the easy axis lies in the plane of the film. If in addition $K_1^{\parallel}>0$ (<0) then the in-plane $\langle 001\rangle$ ($\langle 011\rangle$) axes are easy, giving square hysteresis loops, while the $\langle 011\rangle$ ($\langle 001\rangle$) axes are hard with saturation field equal to $2K_1^{\parallel}/M$. If the magnetization lies in the film plane, perhaps because of the influence of a static applied field, as will be the case in this study, then in-plane MOKE and BLS are sensitive only to the value of $K_1^{\parallel}$ and so from now on we will refer to the value of $K_1^{\parallel}$ simple as K_1.

The BLS experiment is sensitive to spin-wave excitations of small but finite wave vector ($\sim 10^5$ cm^{-1}). In calculating the relevant mode frequencies it is generally necessary to include the effects of dipolar interactions by solving the magnetostatic Maxwell equations and the torque equation of motion of the magnetization simultaneously.[75] However for ultrathin films one may approximate the dipolar interactions with effective field terms in the torque equation.[76] If we assume that the magnetization and in-plane applied field are aligned, and this will be the case for our measurements with the field applied parallel to the easy and hard axes, then the spin-wave frequency is given by

$$\left(\frac{\omega}{\gamma}\right)^2 = \left[H + \frac{2K_1}{M}\cos(4\varphi) + 2\pi D M k_{\parallel} d + \frac{2A}{M}k_{\parallel}^2 \right] \times \left[H + (4\pi M)_{\text{eff}} + \frac{K_1}{M}[1+\cos^2(2\varphi)] - 2\pi D M k_{\parallel} d + \frac{2A}{M}k_{\parallel}^2 \right], \quad (3)$$

in which ω is the circular frequency, γ is the gyromagnetic ratio, φ is the angle between the field and the [001] axis, and

A is the exchange constant. The quantity $k_{\parallel}$ is the in-plane component of the spin-wave vector which is equal to $(2\pi/\lambda)\sin\theta$, in which $\lambda = 5145$ Å is the wavelength of the Ar^+ ion laser, and $\theta = 47°$ is the angle at which the incoming laser beam is incident upon the sample. The last term in each of the square brackets on the right-hand side of Eq. (3) is due to the exchange interaction, while the next to last term is due to the dipolar interactions.

Although enhanced moments and reduced Curie temperatures may occur as discussed in the Introduction to this paper, we are not able to measure the Fe moment directly during our *in situ* experiments. In this study we assume that the room-temperature magnetization is thickness independent and equal to the bulk value of 1710 emu/cm^3. The assumption of a different value would lead to a simple rescaling of deduced anisotropy constants. All BLS calculations also assume the bulk Fe values of 2.09 for the g factor and 2×10^{-6} erg/cm for A, the exchange constant. We see then that the exchange field term in Eq. (3) has a value of 17 Oe, while the dipolar term has a value of 128 Oe for a 10 ML thick film. These terms are non-negligible and cannot be ignored. However by measuring the spin-wave frequency with the field applied parallel to the [001] and [011] in-plane axes, that is with $\varphi = 0°$ and 45°, respectively, we may deduce the values of both K_1 and K_s for a particular value of the film thickness.

III. GROWTH AND STRUCTURE

Growth studies have been carried out using two commercially obtained single-crystal Ag(100) substrates.[77] The first crystal, crystal 1, was mechanically polished to a 0.25 μm diamond paste and then chemically polished and electropolished following the recipe used by Qiu, Person, and Bader.[39] The second crystal was mechanically polished to a 1 μm alumina paste and then electropolished.[78] Once inside the UHV chamber, cycles of 500 eV Ar^+ ion sputtering and annealing to 550 °C were used to initially clean the substrate and to remove the deposited film at the end of each growth run. We observed that the RHEED patterns from crystal 1 were sharper than those from crystal 2 and that the RHEED pattern from crystal 1 became broader after repeated growth runs, as will be described in the next section. This was possibly due to the different polishing procedures used. The base pressure in the chamber prior to growth was better than 2×10^{-10} mbar, typically rising to 5×10^{-10} mbar during deposition. RHEED intensity oscillations were observed during the homoepitaxial growth of Ag onto crystal 1 and also during the growth of Fe onto crystal 2. This allowed us to calibrate a quartz crystal oscillator placed in the sample position and so, by correcting for the different densities, to calibrate the rate for other materials for which we did not make a study of RHEED intensity oscillations. A deposition rate of the order of 1 Å per minute was used for all growth runs.

The design of the sample holder was such that we were unable to simultaneously heat the substrate and perform RHEED measurements. Deposition of the Fe, Ag, and Cr was carried out at ambient temperature (which we loosely refer to as room temperature), normally about 70 °C, which we believe is sufficiently low that only limited interdiffusion of the Fe and Ag should occur.[18,20] RHEED patterns were recorded by means of a CCD camera. In an earlier brief report[79] we reported the growth of two 13.9 ML films on crystal 1. Typical RHEED patterns obtained from the surface of a clean Ag crystal and a 13.9 ML Fe film were presented in Fig. 1 of Ref. 79. These show that the substrate is flat and well ordered and confirm the epitaxial nature of the Fe film.

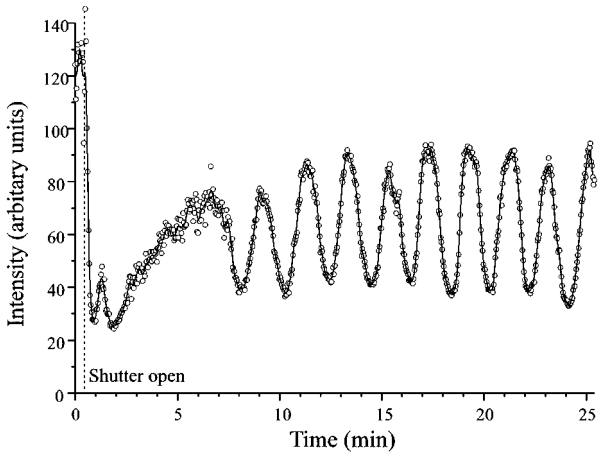

FIG. 1. Intensity oscillations for the 15 keV RHEED specular spot are plotted against deposition time for the growth of Fe on Ag(100) crystal 2. The RHEED beam was aligned some 5° from an in-plane ⟨001⟩ Fe azimuth at a grazing angle of 0.15°.

RHEED patterns were also obtained from Fe films both before and after post-deposition annealing but no significant change was observed. RHEED intensity oscillations were monitored by recording line profiles through the specular RHEED spot as the film was grown. The plotted intensity corresponds to the height of a Gaussian fitted to the line profile. The RHEED beam was misaligned from the [001] azimuth of the Ag substrate by about 5° so that Kikuchi lines did not contribute to the specular spot intensity. Figure 1 shows the variation of the peak intensity of the specular spot during the deposition of Fe onto crystal 2, with the electron beam incident at a grazing angle of about 0.15°. We see that there is a large initial transient and that clear oscillations can be observed once the film thickness exceeds a value of about 4 ML, as has been observed by other researchers.[20,25–27] It is encouraging that these oscillations appear to be undamped but a detailed investigation of experimental factors such as beam stability, choice of position of line profile, and choice of azimuth is required before they can be used to infer the growth mode of the Fe. RHEED intensity oscillations were also observed in the first anti-Bragg position. Both the width and the peak intensity of the specular spot were found to oscillate as a function of the film thickness, although the intensity oscillations were of smaller amplitude than those observed at grazing incidence.

LEED patterns were taken at different stages of the growth of the Fe film and recorded with a CCD camera. Figure 2 shows the evolution of the intensity along a line profile through the Fe(10) [Ag(10)] spot, for a growth on crystal 2. This clearly shows that the diffraction pattern is weakest for an Fe thickness of a little over 3 ML, as previously observed by other researchers.[12–18] There was no observable splitting of either the LEED spots or the RHEED streaks indicating a lack of correlation between step edges up

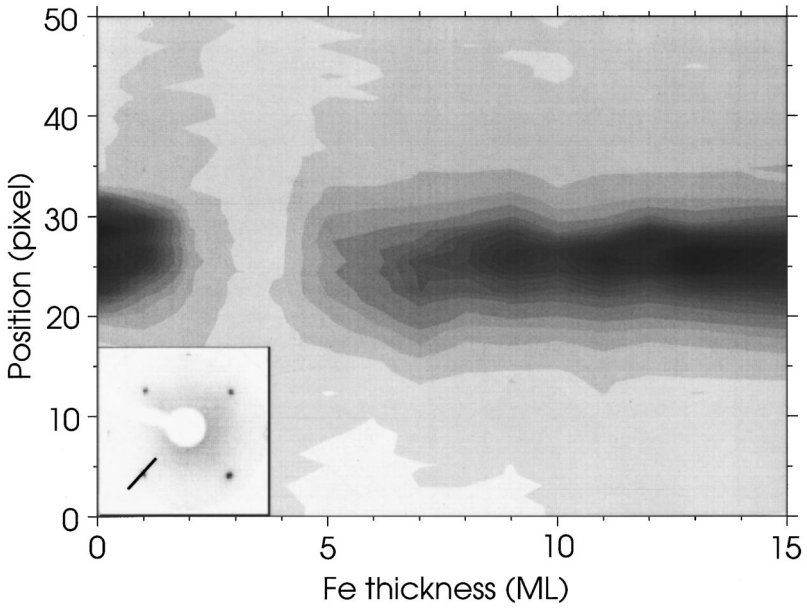

FIG. 2. The intensity line scan through the 66 eV Fe(10) LEED spot is plotted as a function of Fe thickness for the growth of Fe on Ag(100) crystal 2. The inset shows how the line section is related to the full LEED pattern.

to the final thickness used. It was found that line profiles through the LEED Fe(10) spots and RHEED (00) streaks were well fitted by Gaussian and Lorentzian line shapes, respectively. The widths of these curves can be related to the average terrace length on the surface of the film. Both the LEED and RHEED profiles showed a strong broadening after the deposition of about 3 ML of Fe before narrowing again with further Fe deposition. From the shape of the LEED spots we estimate that the average step separation was approximately 80 Å for the Ag substrate, 25 Å after the deposition of 3 ML of Fe, and again about 80 Å after the deposition of 5 ML of Fe.

The profile of the LEED spots and RHEED streaks was monitored during the deposition of Cr and Ag overlayers onto 13.9 ML Fe films grown on crystal 2. Though the absolute RHEED and LEED linewidths are not directly comparable due to the very different geometries of the two techniques, differences in the way the linewidth changes in each technique may be significant. The deposition of Cr was found to have little effect upon the RHEED and LEED linewidths, the average step separation remaining at a value of about 100 Å, as determined from the LEED, for that particular growth run. The deposition of Ag was however found to have a qualitatively different effect. The RHEED linewidth was found to increase by a factor of about 3 with the deposition of about 2 ML of Ag before returning to its original value for a Ag thickness of about 3 ML, after which it slowly increased again. On the other hand, the LEED linewidth was found to remain constant for the first 3 ML of Ag growth before then trebling in size, thus indicating a dramatic decrease in step separation or increase in defect density. It seems that the RHEED and LEED linewidths show opposite trends for the growth of Ag on Fe, while they are similar for the growth of Fe on Ag. We believe that this may be due to the different amount of intermixing and different sensitivities of the LEED and RHEED techniques. The RHEED streaks break up in a manner indicative of a reduction in long-range order. The RHEED spot width was measured across the specular spot and away from the anti-Bragg condition, so direct correlation with step width does not apply. Since the lattice parameter of Cr is closely matched to that of Fe there will be far fewer dislocations in Cr overlayers compared to Ag overlayers, where there is a significant vertical lattice mismatch. While one would expect the diffraction spot widths to be little changed by the growth of Cr on Fe, there might be a significant change for the growth of Ag on Fe. This is indeed what we see, although the reasons for the different evolution of the RHEED and LEED spot widths for the Ag growth are complicated possibly being due to differences in disorder on the different length scales over which RHEED and LEED are sensitive.

IV. THICKNESS DEPENDENCE OF FE ANISOTROPY AND PERPENDICULAR MAGNETIZATION

In order to investigate the thickness dependence of the magnetic anisotropy, BLS and MOKE measurements were performed after the deposition of each monolayer of the Fe film. No magnetic signal was ever observed for values of d less than 3 ML, while the first magnetic signal was normally observed when d was equal to either 3 or 4 ML, there being some variation between different growth runs. Figure 3 shows the MOKE loops obtained from two consecutive growth runs on crystal 2 during which the sample orientation was fixed so that the magnetic field was parallel first to a $\langle 001 \rangle$ and then second to a $\langle 011 \rangle$ Fe axis. It is immediately apparent that the two growth runs were not exactly equivalent since the onset of ferromagnetic order appears to occur earlier for the run in which the field was applied parallel to a Fe$\langle 011 \rangle$ axis. We see that the $\langle 011 \rangle$ axis of the Fe becomes increasingly hard as d is increased while the loop for the $\langle 001 \rangle$ axis remains square as expected for an easy axis.

BLS data obtained from two growth runs on crystal, in which a 13.9 ML film was capped with a Cr overlayer, was presented in Fig. 2 of Ref. 79. While we will discuss the effect of the Cr overlayer later we note now that the mode frequencies increase monotonically during the growth of the Fe layer, and that the difference between the easy [001] and hard [011] axis frequencies also increases monotonically. The corresponding values of the anisotropy constants K_1 and

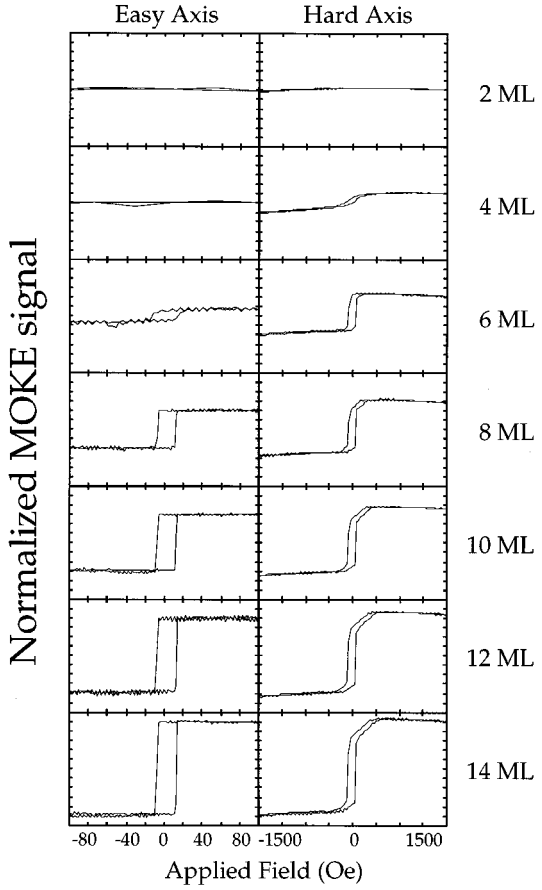

FIG. 3. The evolution of the MOKE hysteresis loop during the growth of Fe on Ag(100) crystal 2 is shown. The left and right columns contain data from two separate growth runs in which the magnetic field was applied parallel to the Fe ⟨001⟩ and ⟨011⟩ axes, respectively. The loops were normalized by scaling the 14 ML loop in each growth run so that its saturation levels were ± 1 and then applying the same scale factor to the other loops. This correctly maintains the relative amplitude of each loop.

K_s were calculated from Eq. (3). The value of K_s is very accurately determined for small values of d and we expect that it will be very sensitive to contamination of the bare Fe surface. In order to quantify this effect we prepared a 6.4 ML Fe film and measured the spin-wave frequency from the bare Fe surface as a function of time with the applied field parallel to an Fe⟨011⟩ axis. The frequencies and the corresponding values of K_s, assuming a constant value of 10^5 erg/cm^3 for K_1 are plotted in Fig. 4. All BLS measurements for a given film thickness are normally completed within 15–20 min after deposition is suspended. We see then that the drift in frequency in this time is negligible and that the value of K_s changes by a few percent at most. We therefore conclude that surface contamination effects play no significant role in our studies.

In Fig. 5 we have plotted the values of K_1 and K_s calculated for 12 different growth runs as a function of d. The error bars shown in Fig. 5 correspond simply to the worst case combination of the hard- and easy-axis frequency errors and as such constitute maximum possible errors in the anisotropy constants. Of course these error bars are only meaningful within the assumptions of the simple model that leads

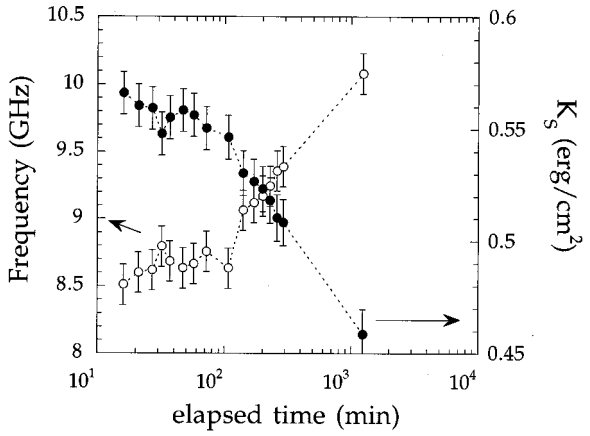

FIG. 4. The measured spin-wave frequencies and the corresponding values of K_s, assuming $K_1 = 10^5$ erg/cm^3, are plotted as a function of the time after the completion of the growth of a 6.4 ML Fe film on Ag(100) crystal 1.

to Eq. (3). The data in Fig. 5 is seen to fall into two sets. The first set contains the first seven (chronologically ordered) growth runs performed on crystal 1, while the second set contains the last three runs performed on crystal 1, one run

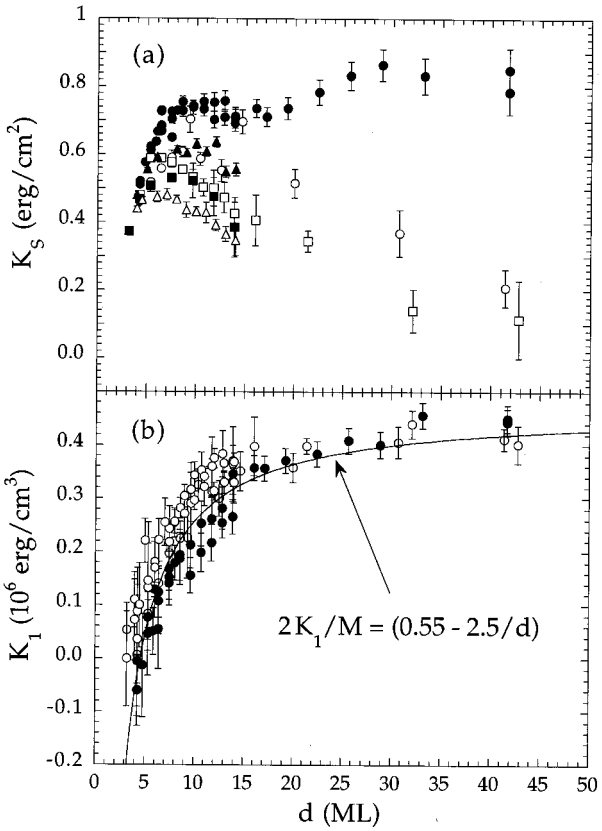

FIG. 5. The values of K_s and K_1 obtained from 12 growth runs are plotted against the Fe thickness d, in (a) and (b), respectively. The closed circles represent data from the first seven growth runs on crystal 1. In (a) the open circles, closed squares, and closed triangles represent three further growth runs on crystal 1, while the open squares and open triangles represent growth runs on Ag/GaAs(100) and Ag(100) crystal 2, respectively. For the sake of clarity these five runs are all represented by open circles in (b).

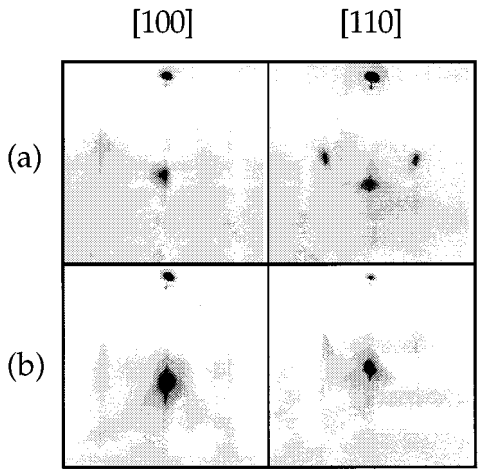

FIG. 6. RHEED patterns from crystal 1 are shown (a) before and (b) after the seventh growth run in which a 40 ML Fe film was deposited. The 15 keV electron beam was parallel to the azimuth indicated in the figure. A grazing angle of approximately 1° was used.

performed on crystal 2, and one run performed on a Ag buffer layer that was grown on a GaAs(100) substrate according to a recipe that has been described previously.[80] During the seventh growth run on crystal 1 a 40 ML Fe film was grown, whereas previously the Fe thickness had never exceeded 14 ML. We observed a systematic difference in the RHEED patterns obtained from the bare crystal 1 before and after the seventh run, examples of which are shown in Fig. 6. For the patterns recorded after the seventh run the {10} RHEED spots are less sharp, while their intensity has decreased relative to that of the specular spot. After the seventh run we see from Fig. 5 that the maximum value of K_s obtained during a growth is reduced while the value of K_s is seen to decrease for large values of d. The value of K_1 is larger for small values of d after the seventh run but for large values of d there seems to be little difference between the two sets of data. We will discuss in Sec. VI how these changes in the values of the anisotropy constants may be explained by an increase in the number of defects on the Ag(100) surface after the deposition and removal by sputtering of the 40 ML Fe film. The fact that the results from the growth run performed on crystal 2 are similar to those obtained after the seventh growth run on crystal 1 is not unexpected, since inferior RHEED patterns were obtained from crystal 2. Within the first seven growth runs on crystal 1 it was found that there was some scatter in the BLS frequencies measured at small Fe thicknesses, but that for larger thicknesses these frequencies were highly reproducible. For the second set of data we have used different symbols in Fig. 5(a) to differentiate between the different growth runs because then it can be seen that within each growth run, for Fe thicknesses greater than about 7 ML, the value of K_s appears to decrease linearly with increasing Fe thickness.

A limited number of growths were performed with substrate temperatures of up to 200 °C but as mentioned previously we were unable to simultaneously obtain RHEED patterns from the Fe surface. A few BLS measurements were performed but it is difficult to relate these to our room-temperature measurements since the temperature dependence of the magnetization and anisotropy in our samples is not presently known. Furthermore cooling to room temperature is a slow process and surface contamination may affect BLS measurements performed once the substrate has cooled. BLS measurements were performed during an annealing treatment of a sample that had been grown at room temperature. The substrate temperature was increased to a maximum value of 200 °C and then allowed to fall slowly back to room temperature, the entire cycle taking some 4 h to complete. The final room-temperature value of K_s for the uncoated Fe film was found to be some 10% larger than the initial value. Since from Fig. 4 surface contamination is expected to have the opposite effect we might conclude that the annealing treatment has a beneficial effect upon the film structure and hence the surface anisotropy constant, as reported by Qiu, Person, and Bader,[39] even though we could observe no noticeable change in the RHEED patterns. Alternatively it is possible that the annealing treatment promotes further interdiffusion at the Fe/Ag interface, hence reducing the magnetic thickness of the film and leading to an apparent increase in the value of K_s. Post-deposition annealing of Fe films grown at room temperature has been reported[38] to give flatter films than growth at elevated temperatures, which in turn are flatter than an unannealed room-temperature growth.

V. OVERLAYER EXPERIMENTS

In Fig. 5 we presented results for the dependence of the anisotropy constants of the Fe film upon its thickness. However these growth runs were often terminated by adding an overlayer of a different material to the completed Fe film. We now consider experiments of this type that were performed before the seventh growth run on crystal 1, that is, before the RHEED patterns from the Ag substrate were observed to deteriorate. Figure 2 of Ref. 79 showed the effect of capping a 13.9 ML Fe film with Cr. Both the easy- and hard-axis frequencies show a small dip with the initial deposition of Cr and this leads to a small peak in K_s at this point. The deposition of Cr also seems to lead to a significant increase in the value of K_1. However, for a Fe film that was approximately 15 ML thick (the thickness is uncertain because the Fe rate became unstable during the growth), the deposition of Cr was again found to produce a peak in the calculated value of K_s but no increase in the value of K_1 was observed. We therefore believe that the initial peak in the value of K_s is a reproducible effect, while the apparent enhancement in the value of K_1 shown in Fig. 2 of Ref. 79 is probably an artifact produced by the pasting together of the two data sets.

Figure 3 of Ref. 79 showed the spin-wave frequencies measured during a growth run in which Ag was deposited onto a 13.9 ML Fe film. The values of the calculated anisotropy constants were again shown and the spin-wave frequency and hence the anisotropy constants vary monotonically as the thickness of the Ag overlayer is increased. Overlayers were also added to somewhat thinner Fe films. Figure 7 shows the effect of adding a Cr overlayer to a 6.4 ML Fe film, while in Fig. 8 a 6 ML Fe film was capped with a Ag overlayer. In this case both Cr and Ag deposition lead to a monotonic decrease in the value of K_s, while the value of K_1 again shows no significant change as the overlayer is

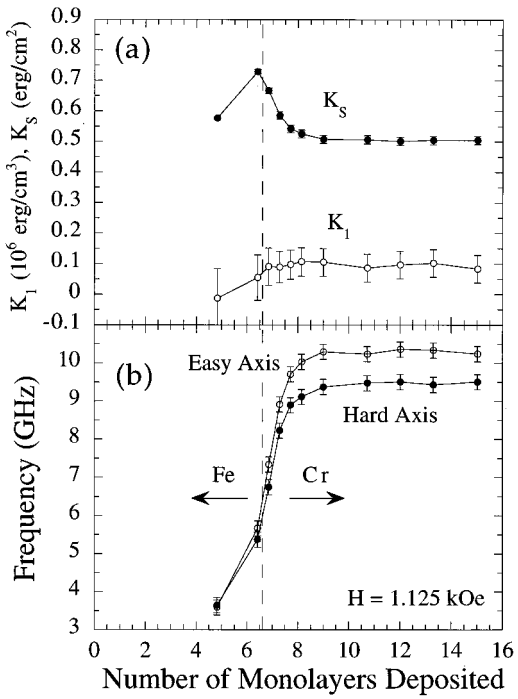

FIG. 7. (a) Values of the surface anisotropy constant K_s and the cubic anisotropy constant K_1 calculated from the data in (b) are shown. (b) The easy- and hard-axis BLS frequencies measured in an experiment in which a 6.4 ML Fe film grown on crystal 1 was capped with Cr are plotted. The frequency error bars are smaller than the symbols used.

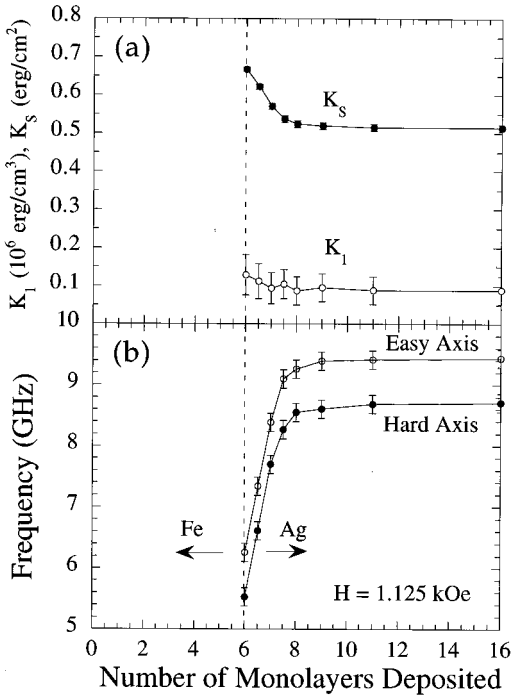

FIG. 8. (a) Values of the surface anisotropy constant K_s and the cubic anisotropy constant K_1 calculated from the data in (b) are shown. (b) The easy- and hard-axis BLS frequencies measured in an experiment in which 6.0 ML Fe film grown on crystal 1 was capped with Ag are plotted. The frequency error bars are smaller than the symbols used.

added. We note that the changes in K_s produced by the overlayers are larger in absolute terms and also as a percentage of the initial K_s value for the case that $d \approx 6$ ML than for the case that $d = 13.9$ ML. However when an overlayer of Ag was added to a 3.2 ML Fe film the decrease in K_s was found to be much smaller being about 6% of the initial value of 0.43 erg/cm^2. This is consistent with the presence of Ag atoms at the upper surface of the Fe film for this thickness.

VI. DISCUSSION

For very small Fe thicknesses our LEED observations are in agreement with those of other researchers and imply that full Fe coverage of the Ag is not achieved until $d \geq 3$ ML. The absence of any magnetic signal here may be because first, intermixing of the Fe and Ag has reduced the Fe moment; second, that our samples are paramagnetic or superparamagnetic at room temperature; or third, that the sample magnetization lies perpendicular to the plane of the film. In the latter case, an in-plane applied field should cant the magnetization towards the film plane. For a single-domain state one would expect to observe a well defined spin-wave mode in the BLS experiment, as has been observed for the case of Fe/Cu(100),[81] and a MOKE signal due mainly to the polar Kerr effect which is much stronger[82] than the longitudinal Kerr effect. However there is now both experimental[62] and theoretical[59] support for the existence of a fine scale domain structure in the vicinity of the RPT. Since the laser spot size is 1–2 mm in the MOKE experiment we would therefore expect no net signal. Also we would expect the modes observed by BLS to be significantly broadened if the domain size were less than the micron scale spin-wave wavelength. We have calculated the effective demagnetizing field given in Eq. (2) from our BLS data and find that this quantity is approximately zero and sometimes slightly negative when a spin-wave mode is first observed. Since we are presently only able to apply a magnetic field parallel to the plane of the sample we are unable to sweep out a perpendicular domain structure and we believe that such a structure is responsible for the absence of a magnetic signal at this point in our experiments.

Let us next compare the values of K_1 and K_s obtained from the first seven growth runs performed upon crystal 1 with those obtained by other authors. The solid curve plotted in Fig. 5 corresponds to the form $2K_1/M = (0.55 - 2.5/N)$ for the in-plane fourfold anisotropy field (measured in kOe) in which N is the number of Fe monolayers. This is the best fit form given by Heinrich and Cochran[3] and it can be seen to be in rather good agreement with our data when we consider that the points in Fig. 5 that lie off the curve correspond to the region in which two data sets have been pasted together. We cannot conclusively say that K_1 becomes negative for Fe thicknesses less than 5 ML although the trend of our data suggests that this might occur. Also from our collected experimental data we have no strong evidence that the value of K_1 is affected by overlayers of either Ag or Cr which is again consistent with the findings of Heinrich and Cochran.[3] From Fig. 5 we see that the value of K_s is strongly thickness dependent for small values of d, before obtaining its maximum value at about $d = 10$ ML, while it varies much less for larger

Fe thicknesses as previously seen.[3] Heinrich and Cochran[3] reported K_s values of 0.81 and 0.96 erg/cm^2 for the Fe/Ag and Fe/vacuum interfaces, respectively, which imply an average value of 0.89 erg/cm^2 for an Fe film with one Ag and one vacuum interface. From Fig. 5 we see that the maximum value of K_s of 0.86 erg/cm^2 measured for a 30 ML Fe thickness comes close to this value but that in general our values are somewhat smaller than this.

We now consider the second set of data in Fig. 5. We see that the rate of decrease of the value of K_s for $d>7$ ML is actually rather similar for the different growth runs in this set although they are clearly offset vertically with respect to one another. The linear dependence of K_s upon d suggests the presence of an easy plane uniaxial perpendicular volume anisotropy field, the strength of which is approximately 4 kOe. This is much larger than the 0.8 kOe magnetoelastic anisotropy field that was calculated by assuming a vertical strain given by the Poisson's ratio for bulk Fe.[49] While the values of K_s in the second set of data are reduced relative to those in the first set of data, the values of K_1 are clearly enhanced. The RHEED patterns in Fig. 6 clearly show that the surface of the Ag substrate was flatter for the first set of data and we therefore expect that the films in the first set were of superior structural quality. A possible explanation for the difference in the magnetic properties between our two sets of data can be found in studies of bcc Ni films[25] in which a network of line defects with fourfold symmetry was found to induce a large in-plane fourfold anisotropy and also a perpendicular uniaxial anisotropy. For the second set of data we suggest that first, the films were rougher, leading to a reduction in the maximum value of K_s, and second, that defects in the films have contributed to both an increase in the value of K_1 and also to a perpendicular uniaxial volume anisotropy.

Let us now consider the results of overlayer experiments performed upon films from the first set of data in Fig. 5. From Fig. 3 of Ref. 79 we see that approximately 3 ML of Ag must be deposited onto a 13.9 ML Fe film before the value of K_s becomes saturated at about 0.56 erg/cm^2. We note that 3 ML of Ag were also required for the RHEED linewidth to narrow which suggests that the gradual change in K_s may be related to the growth mode of the Ag rather than being a purely electronic effect. If we assume that the upper and lower Fe/Ag interfaces are identical in terms of their surface anisotropy constant, and this need not be the case, then we deduce surface anisotropy values of 0.56 erg/cm^2 for the Fe/Ag interface and 0.84 erg/cm^2 for the Fe/vacuum interface which are again somewhat smaller than those reported by Heinrich and Cochran.[3] From Fig. 2 of Ref. 79 we see that, with the deposition of Cr, the value of K_s increases from a value of about 0.71 to 0.77 erg/cm^2 before decreasing to 0.61 erg/cm^2. This nonmonotonic behavior of K_s corresponds to the small dip seen in both the hard- and easy-axis spin-wave frequencies, which has been observed repeatedly in our BLS experiments. Our structural studies show that the LEED and RHEED linewidths are not greatly affected by the deposition of Cr onto Fe, suggesting that the surface of the film is not roughened as Cr is deposited. The nonmonotonic variation of K_s may therefore be associated with an antiferromagnetic ordering of successive layers of Cr moments in the first few ML of Cr. This order is however expected to be quickly frustrated with increasing Cr thickness due to the influence of interfacial roughness.[8] The results of capping experiments performed on thinner Fe layers, shown in Figs. 7 and 8, are qualitatively similar to those just discussed except that a monotonic evolution of K_s is now observed in the Cr capping experiment. At present it is unclear why a different behavior should be observed. This might be due to the different role played by quantum well states for the two Fe layer thicknesses. Alternatively the difference in the magnetic properties may be due to a difference in structure. However the LEED and RHEED linewidths for the completed Fe surface were not noticeably different for the two Fe thicknesses used which would indicate the sensitivity of magnetic properties to minor changes in structure.

In conclusion we have shown that the values of the anisotropy constants K_1 and K_s in Fe/Ag(100) films are strongly dependent upon the Fe layer thickness and that they are also highly sensitive in different ways to the surface quality of the Ag substrate. Indeed the thickness dependence of K_s has been shown to be qualitatively different for growth on inferior substrates. Capping experiments have shown that while the value of K_1 is insensitive to the presence of the capping material, the value of K_s is strongly affected with its value saturating after the deposition of about 3 ML of overlayer. Furthermore, Ag and Cr capping layers have been shown to have a qualitatively different effect upon the value of K_s. We suggest that the nonmonotonic dependence of K_s upon the thickness of a Cr overlayer may be due to magnetic order within the Cr. Further experiments are now required to quantify the exact relationship between structure and magnetism in these structures.

ACKNOWLEDGMENTS

We would like to acknowledge the financial support of the EPSRC and the DRA and useful discussions with M. Kowalewski and Professor B. Heinrich.

*Permanent address: The Department of Physics, University of Exeter, Stocker Road, Exeter EX4 4QL, UK.

[1] L. Néel, J. Phys. Radium **15**, 225 (1954).
[2] R. J. Hicken and G. T. Rado, Phys. Rev. B **46**, 11 688 (1992).
[3] B. Heinrich and J. F. Cochran, Adv. Phys. **42**, 523 (1993).
[4] B. Hillebrands, J. Fassbender, R. Jungblut, G. Güntherodt, D. J. Roberts, and G. A. Gehring, Phys. Rev. B **53**, 10 548 (1996).
[5] S. S. P. Parkin, N. More, and K. P. Roche, Phys. Rev. Lett. **64**, 2304 (1990).
[6] J. Unguris, R. J. Celotta, and D. T. Pierce, Phys. Rev. Lett. **69**, 1125 (1992).
[7] C. Turtur and G. Bayreuther, Phys. Rev. Lett. **72**, 1557 (1994).
[8] D. Stoeffler and F. Gautier, J. Magn. Magn. Mater. **147**, 260 (1995).
[9] W. R. Tyson and W. A. Miller, Surf. Sci. **62**, 267 (1977).
[10] I. Z. Mezey and J. Giber, Jpn. J. Appl. Phys. **11**, 1569 (1982).
[11] P. Etienne and J. Massies, J. Phys. (France) III **3**, 1581 (1993).
[12] G. C. Smith, H. A. Padmore, and C. Norris, Surf. Sci. **119**, L287 (1982).
[13] J. Araya-Pochet, C. A. Ballentine, and J. L. Erskine, Phys. Rev. B **38**, 7846 (1988).
[14] H. Li and B. P. Tonner, Phys. Rev. B **40**, 10 241 (1989).

[15] B. T. Jonker, K. Walker, E. Kisker, G. A. Prinz, and C. Carbone, Phys. Rev. Lett. **57**, 142 (1986).
[16] H. Li, Y. S. Li, J. Quinn, D. Tian, J. Sokolov, F. Jona, and P. M. Marcus, Phys. Rev. B **42**, 9195 (1990).
[17] F. Ciccacci, G. Chiaia, and S. De Rossi, Solid State Commun. **88**, 827 (1993).
[18] S. De Rossi and F. Ciccacci, Surf. Sci. **307–309**, 496 (1994).
[19] J. Chen, M. Drakaki, and J. L. Erskine, Phys. Rev. B **45**, 3636 (1992).
[20] P. J. Schurer, Z. Celinski, and B. Heinrich, Phys. Rev. B **51**, 2506 (1995).
[21] H. Tang, M. D. Wieczorek, D. J. Keavney, D. F. Storm, and J. C. Walker, J. Magn. Magn. Mater. **104–107**, 1705 (1992).
[22] W. F. J. Egelhoff, in *Ultrathin Magnetic Structures I*, edited by J. A. C. Bland and B. Heinrich (Springer, Berlin, 1994).
[23] B. Heinrich, K. B. Urquhart, A. S. Arrot, J. F. Cochran, K. Myrtle, and S. T. Purcell, Phys. Rev. Lett. **59**, 1756 (1987).
[24] B. Heinrich, Z. Celinski, J. F. Cochran, A. S. Arrott, K. Myrtle, and S. T. Purcell, Phys. Rev. B **47**, 5077 (1993).
[25] B. Heinrich, S. T. Purcell, J. R. Dutcher, K. B. Urquhart, J. F. Cochran, and A. S. Arrott, Phys. Rev. B **38**, 12 879 (1988).
[26] Z. Celinski and B. Heinrich, J. Magn. Magn. Mater. **99**, L25 (1991).
[27] Z. Q. Qui, J. Pearson, and S. D. Bader, Phys. Rev. B **49**, 8797 (1994).
[28] S. T. Purcell, A. S. Arrott, and B. Heinrich, J. Vac. Sci. Technol. B **6**, 794 (1988).
[29] J. A. Stroscio, D. T. Pierce, and R. A. Dragoset, Phys. Rev. Lett. **70**, 3615 (1993).
[30] J. A. Stroscio and D. T. Pierce, Phys. Rev. B **49**, 8522 (1994).
[31] W. F. J. Egelhoff and I. Jacob, Phys. Rev. Lett. **62**, 921 (1989).
[32] J. W. Evans, D. E. Sanders, P. A. Thiel, and A. E. DePristo, Phys. Rev. B **41**, 5410 (1990).
[33] J. W. Evans, Phys. Rev. B **43**, 3897 (1991).
[34] J. A. Stroscio, D. T. Pierce, M. D. Stiles, A. Zangwill, and L. M. Sander, Phys. Rev. Lett. **75**, 4246 (1995).
[35] K. Thürmer, R. Kock, M. Weber, and K. H. Rieder, Phys. Rev. Lett. **75**, 1767 (1995).
[36] M. C. Bartelt and J. W. Evans, Phys. Rev. Lett. **75**, 4250 (1995).
[37] M. Stampanoni, A. Vaterlaus, M. Aeschlimann, and F. Meier, Phys. Rev. Lett. **59**, 2483 (1987).
[38] D. Bürgler, C. M. Schmidt, T. M. Schaub, and H.-J. Güntherodt (unpublished).
[39] Z. Q. Qiu, J. Person, and S. D. Bader, Phys. Rev. Lett. **70**, 1006 (1993).
[40] S. Ohnishi, M. Weinert, and A. J. Freeman, Phys. Rev. B **30**, 36 (1984).
[41] R. Richter, J. G. Gay, and J. R. Smith, Phys. Rev. Lett. **54**, 2704 (1985).
[42] J. A. C. Bland, R. D. Bateson, B. Heinrich, Z. Celinski, and H. J. Lauter, J. Magn. Magn. Mater. **104–107**, 1909 (1992).
[43] J. A. C. Bland, C. Daboo, B. Heinrich, Z. Celinski, and R. D. Bateson, Phys. Rev. B **51**, 258 (1995).
[44] C. L. Wooten, J. Chen, G. A. Mulhollan, J. L. Erskine, and J. T. Markert, Phys. Rev. B **49**, 10 023 (1994).
[45] B. Heinrich, K. B. Urquhart, J. R. Dutcher, S. T. Purcell, J. F. Cochran, A. S. Arrott, D. A. Steigerwald, and W. F. Egelhoff. Jr, J. Appl. Phys. **63**, 3863 (1988).
[46] N. C. Koon, B. T. Jonker, F. A. Volkening, J. J. Krebs, and G. A. Prinz, Phys. Rev. Lett. **59**, 2463 (1987).
[47] J. G. Gay and R. Richter, Phys. Rev. Lett. **56**, 2728 (1987).
[48] R. Cabanel, P. Etienne, S. Lequien, G. Creuzet, A. Bartélémy, and A. Fert, J. Appl. Phys. **67**, 5409 (1990).
[49] B. Heinrich, Z. Celinski, J. F. Cochran, A. S. Arrott, and K. Myrtle, J. Appl. Phys. **70**, 5769 (1991).
[50] P. J. Jensen and K. H. Bennemann, Phys. Rev. B **42**, 849 (1990).
[51] R. P. Erickson and D. L. Mills, Phys. Rev. B **44**, 11 825 (1991).
[52] R. P. Erickson and D. L. Mills, Phys. Rev. B **46**, 861 (1992).
[53] D. Pescia and V. L. Pokrovsky, Phys. Rev. Lett. **65**, 2599 (1990).
[54] R. P. Erickson and D. L. Mills, Phys. Rev. B **43**, 11 527 (1991).
[55] A. Berger and H. Hopster, Phys. Rev. Lett. **76**, 519 (1996).
[56] Y. Yafet and E. M. Gyorgy, Phys, Rev. B **38**, 9145 (1988).
[57] A. Kashuba and V. L. Pokrovsky, Phys. Rev. Lett. **78**, 3155 (1993).
[58] A. Kashuba and V. L. Pokrovsky, Phys. Rev. B **48**, 10 335 (1993).
[59] Ar. Abanov, V. Kalatsky, V. L. Pokrovsky, and W. M. Saslow, Phys. Rev. B **51**, 1023 (1995).
[60] A. Moschel and K. D. Usadel, Phys. Rev. B **49**, 12 868 (1994).
[61] S. T. Chui, Phys. Rev. Lett. **74**, 3896 (1995).
[62] A. Berger and H. Hopster, J. Appl. Phys. **79**, 5619 (1996).
[63] J. E. Ortega and F. J. Himpsel, Phys. Rev. Lett. **69**, 844 (1992).
[64] A. Carl and D. Weller, Phys. Rev. Lett. **74**, 190 (1995).
[65] D. Venus and B. Heinrich, Phys. Rev. B **53**, R1733 (1996); B. Heinrich, J. F. Cochran, D. Venus, K. Totland, D. Atlan, S. Govorkov, and K. Myrtle, J. Appl. Phys. **79**, 4518 (1996).
[66] A. Davies, J. A. Stroscio, D. T. Pierce, and R. J. Celotta, Phys. Rev. Lett. **76**, 4175 (1996).
[67] P. Beauvillain, A. Bounouh, C. Chappert, R. Mégy, S. Ould-Mahfoud, J. P. Renard, P. Veillet, and D. Weller, J. Appl. Phys. **76**, 6078 (1994).
[68] B. N. Engel, M. H. Wiedmann, and C. M. Falco, J. Appl. Phys. **75**, 6401 (1994).
[69] J. Kohlhepp and U. Gradmann, J. Magn. Magn. Mater. **139**, 347 (1995).
[70] M. H. Wiedmann, C. Marliere, B. N. Engel, and C. M. Falco, J. Magn. Magn. Mater. **148**, 125 (1995).
[71] B. Hillebrands, P. Baumgart, and G. Güntherodt, Phys. Rev. B **36**, 2450 (1987).
[72] A. Ercole, R. J. Hicken, C. Daboo, M. Gester, and J. A. C. Bland (unpublished).
[73] TFPDAS3, Professor B. Hillebrands, University of Kaiserslautern, Germany.
[74] H. J. G. Draaisma and W. J. M. de Jonge, J. Appl. Phys. **64**, 3610 (1988).
[75] R. W. Damon and J. R. Eschbach, J. Phys. Chem. Solids **19**, 308 (1961).
[76] J. F. Cochran, J. Rudd, W. B. Muir, B. Heinrich, and Z. Celinski, Phys. Rev. B **42**, 508 (1990).
[77] Metals, Crystals and Oxides Ltd, Harston, Cambridge CB2 5NX, United Kingdom.
[78] M. Kowalewski and B. Heinrich (private communication).
[79] R. J. Hicken, A. Ercole, S. J. Gray, C. Daboo, and J. A. C. Bland, J. Appl. Phys. **79**, 4987 (1996).
[80] R. J. Hicken, C. Daboo, M. Gester, A. J. R. Ives, S. J. Gray, and J. A. C. Bland, J. Appl. Phys. **78**, 6670 (1995).
[81] J. R. Dutcher, J. F. Cochran, I. Jacob, and W. F. Egelhoff Jr., Phys. Rev. B **39**, 10 430 (1989).
[82] S. D. Bader, D. Li, and Z. Q. Qui, J. Appl. Phys. **76**, 6419 (1994).